INSTITUTE OF PHYSICS PUBLISHING SMART MATERIALS AND STRUCTURES

Smart Mater. Struct. **11** (2002) 854–862 PII: S0964-1726(02)39925-7

A feasibility study of active vibration isolation using THUNDER actuators

J P Marouzé[1] **and L Cheng**[2]

[1] Department of Mechanical Engineering, Laval University, Québec, Canada G1K 7P4
[2] Department of Mechanical Engineering, The Hong Kong Polytechnic University, Hung Hom, Kowloon, Hong Kong, China

E-mail: mmlcheng@polyu.edu.hk

Received 10 October 2001, in final form 28 May 2002
Published 2 October 2002
Online at stacks.iop.org/SMS/11/854

Abstract
The 'thin layer composite unimorph piezoelectric driver and sensor' (THUNDER) piezoelectric actuator is a newly developed active control device that possesses many advantages over other conventional piezoelectric actuators. Particularly, its capacity for generating high displacement and its inherent flexibility make it an ideal candidate in applications for active vibration isolation. In this paper, we focus on the simulation, design and experimental tests of a hybrid isolation system by taking advantage of both the passive and active effects provided by THUNDER actuators. Different aspects concerning its practical use are first investigated. Then its dynamic properties are modelled using a mechatronic approach. From there a dynamic model is established considering the parameter evolution due to the mass loading. Finally a simple prototype is designed using three THUNDER actuators. Both simulation and experimental tests show the potential of THUNDER actuators in active vibration control applications.

(Some figures in this article are in colour only in the electronic version)

1. Introduction

In the last decade, technologies using smart materials have become the enabler that cuts across traditional boundaries in material science and engineering. Smart technology, including sensors, actuators and controllers, has given rise to a broad spectrum of research and applications. Among other factors, a successful implementation of the smart system strongly relies on the development of actuators of high performance. As a first step in a long-term research programme, aiming at controlling vibrations of floor panels in an airplane, the use of a new generation of actuators has been investigated. In this paper, we focus on the development, simulations and tests of a simplified prototype to achieve an active isolation system.

Aircraft active control using smart materials has been a hot topic during the past few years. As typical examples, one can mention active boundary layer control [1], structural vibration control [2–5] as well as interior noise reduction [6]. As far as vibration and noise control are concerned, piezoelectric devices have proved themselves to be one of the most promising actuators. Bonded directly on the structure surface, they can be used both as sensors and actuators. The use of surface-bonded actuators is designed to control the flexible motion of the structure, and turns out to be ineffective when the structure undergoes a rigid body motion, which is significant in some parts of the aircraft such as floor panels. In these cases, active isolation should be implemented between the floor and the supporting structure.

Numerous publications have reviewed smart materials from an application oriented state-of-the-art point of view [7]. Basically, six categories of actuators have been widely investigated and used: electrodynamic actuators [8], hydraulic systems [9], piezoelectric elements [10] or magnetostrictive actuators [8], electro-active polymers [11] and shape memory alloys (SMAs) [12]. Electrodynamic actuators are normally cheap but are bulky and heavy for the force they can generate. Hydraulic actuators can provide very high forces but are expensive, heavy and inefficient at high frequencies. Classical piezoceramic or magnetostrictive actuators provide very limited displacement. As mentioned in a very recent paper [13], monolithic piezoelectric actuators can generate massive stress ($\sim$tons/inch^2) but only nimiscale

strain ($\sim 10^{-3}$). A proper design of mechanical amplification system is usually needed to increase the displacement generation at the expense of reducing the force loading capacity. Electro-active polymers and SMAs are able to provide high displacement, their dynamic response is however limited to rather low-frequency range.

Due to the aforementioned drawbacks, all these classical actuators seem to be difficult to use in our applications. Alternatives should be investigated using high displacement actuators to develop an active isolation system for in-flight application. The exploration for large-displacement actuators has attracted the attention of some researchers, as evidenced by a very recent paper [13]. Piezo-composite curved actuators seem to provide some attractive properties for vibration applications. A typical example is the recent work by Malowichi and Leo [14], in which such actuators were used for automotive seat suspensions via feedback control. Both simulations and experiments on a four-degree-of-freedom model have shown encouraging results. In this paper, the possibilities of using the newly developed 'thin layer composite unimorph piezoelectric driver and sensor' (THUNDER) for vibration isolation are investigated. The THUNDER is manufactured to deform out-of-plane when under an applied voltage, and exhibits much larger displacement than other piezoceramic actuators. The pursuit of a large displacement with reasonably good load-bearing capacity is the main reason why the THUNDER is chosen for this particular application. Moreover, due to its particular fabrication process [15], both passive and active isolation may be obtained. Before designing an active isolation system for aircraft, it is necessary to carry out a feasibility study using a simple system.

Active vibration isolation using classical actuators associated with various control algorithms is covered adequately in the literature. A summary can be found in [16]. The present work does not claim to provide any contribution in this regard. Instead, emphasis is on investigating different aspects related to the use of THUNDER actuators for isolation purposes. Firstly, THUNDER installation is presented, aimed at obtaining the maximum displacement. Then, on the basis of a mechatronic approach, a simple model is developed combining both the passive and active effects of the THUNDER. This model is then used to design an isolation system and to study the performance of feedback control. Finally, experimental tests are performed using an isolation prototype to demonstrate the feasibility of vibration isolation using the THUNDER. Wherever possible, experimental results are compared to numerical simulations. It can be shown that an effective isolation of the high-frequency components is ensured by the flexibility of the THUNDER, whilst an active feedback controller can effectively improve the low-frequency isolation by reducing the fundamental natural frequency of the system.

2. THUNDER actuator and its installation

The high displacement range and the high load capacity provided by THUNDER actuators result from its particular fabrication process [15]. This actuator uses an ultra-high performance hot melt adhesive, LaRC^{TM}–SI, to bond metal foils to PZT ceramic at elevated temperatures in order to create a pre-stressed condition when cooled to room temperature. The differences in the thermal expansion coefficients of the various bonded layers make up the composite laminate, and offer the THUNDER special characteristics. Various applications using the THUNDER have been investigated by NASA Langley Research Center. Typical examples include aeroelastic response control and airfoil shaping [17], speakers and noise control through walls of aircraft fuselage, etc. Meanwhile, research using different metallic substrates as hosts has also been carried out. Two appealing features motivated the choice of THUNDER actuators in our pursued application. The first is its high displacement capacity. As is known, high amplitude vibrations usually occur at low frequencies and classical piezoelectric actuators cannot impose sufficient motion to the system even under high voltage. The second feature is that the THUNDER is a natural all-in-one semi-active actuator, made of one passive and one active part. The passive isolation effects come from the flexibility provided by the curved stainless-steel plate used as the host of piezoceramics. It acts like a spring to allow the THUNDER to reach a good loading capacity on one hand, and to provide a classical isolation effect at high frequencies on the other hand. An active controller can then be added to control the THUNDER motion to achieve an effective active isolation.

A proper installation of the THUNDER actuator is a key factor to fully explore its high displacement feature. A series of tests were performed in our laboratories to find the best attachment between the actuator and its supporting parts. In every test, the THUNDER was driven by an ac voltage and the output was the apex velocity or displacement with and without a mass on it. Responses to different frequencies and to the narrow-band white noise were analysed. Excitation signals were generated using a B&K 3550 signal analyser and amplified using a 100 gain high-voltage amplifier built with APEX PA89 high voltage amplifiers. An Ometron VS-100 laser vibrometer was used to measure the velocity of the THUNDER apex when there was no load on the THUNDER apex. When a mass was applied on its apex, a B&K 4508 Deltatron accelerometer was used to measure displacement through integration with a B&K Nexus conditioning amplifier. Acquired signals were sent to the analyser with an I/O data board for identification and analysis.

The THUNDER was installed in four different ways: clamped, fixed with tight or loose screws and finally both ends fixed with silicone. A 250 g mass was applied on the THUNDER apex, and the mass was fixed to the apex using silicone gels as illustrated in figure 1. During experiments, a 200 V (root mean square (rms)) signal varying from 5 to 100 Hz was applied to the piezoelectric. Similar observations were obtained for all frequencies tested. Figure 2 shows a typical variation of the apex displacement with respect to voltage at 15 Hz for each installation. It can be seen that the nearly free–free condition (using loose screws) allows the highest displacement range. It was found however that skipping would occur at frequencies higher than 30 Hz. It is therefore not practical to use in any real applications. A tighter installation using tight screws reduces the performance and the clamped installation gives the smallest motion among all four cases considered. The best installation method was that

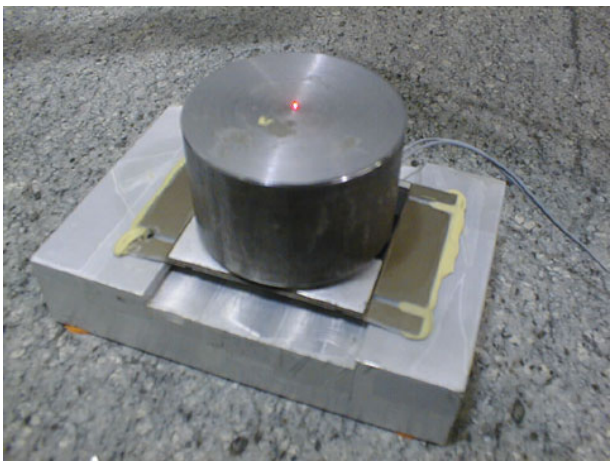

Figure 1. The THUNDER with 500 g load on the apex and with both ends fixed with silicone gels.

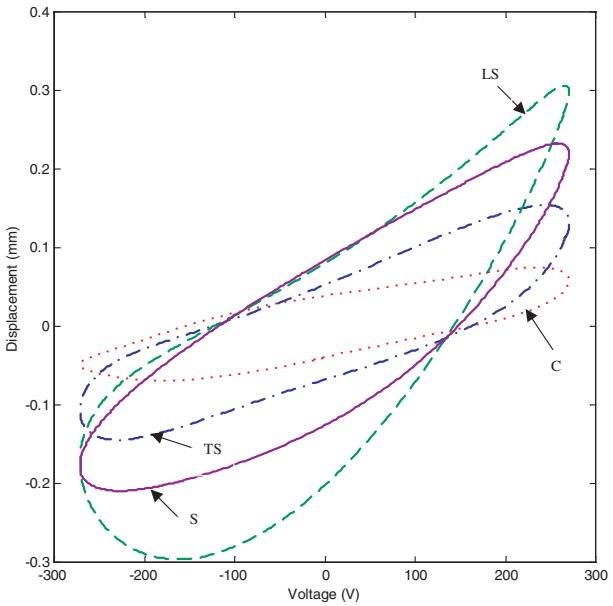

Figure 2. Displacement versus voltage under different boundary conditions: TS, tight screw; LS, loose screw; C, clamped; S, silicone gels (200 V rms harmonic excitation applied to the THUNDER at 15 Hz with 500 g on the THUNDER apex).

using silicone gels at both ends, which provided reasonably large displacement without skipping. It is therefore a good compromise between displacement and feasibility in industrial applications. This configuration is used in other tests reported hereafter. It should also be mentioned that hysteresis is relatively high with the silicone gel as shown in figure 2. It is anticipated that the situation would be more critical if applications at high frequencies were perused. In our case, the active effect was expected only at low frequencies (with the use of a low pass filter below 150 Hz), and the hysteresis observed could be handled by feedback controllers.

3. System modelling and identifications

There are different ways to model a THUNDER actuator depending on the application and precision necessary to understand the dynamic behaviour of the actuator: the Thévenin equivalent model [18], the continuum model [19] and the finite element model [20]. Traditional continuum mechanic theory is based on multilayer thin shell modelling. This modelling process provides good results when no load is applied on the actuator apex [19]. Its extension to the loaded actuator modelling is not straightforward, since one of the fundamental assumptions is that stress components normal to the middle surface are small compared with the other stress components and therefore may be neglected in the stress–strain relation. Moreover, the relation between the tension applied to the piezoelectric device and the apex displacement is found to be nonlinear and therefore cannot be directly used for classical control design. Due to the large displacement of the THUNDER, it is impractical to perform any linearization. A finite element model (FEM) is more versatile. It has been used in the past to achieve a better understanding of the system and to optimize the design of actuators [20]. It is however difficult to implement control design in the FEM, as illustrated by many researchers [1]. In the present research, the focus is not on the accurate modelling of the THUNDER actuator. Instead we want to consider the THUNDER dynamics and include this as a component of a whole control system. Therefore, a simple and flexible model is needed to help design the isolation and the implementation of the controller. All these reasons justify the use of the Thévenin equivalent model [18].

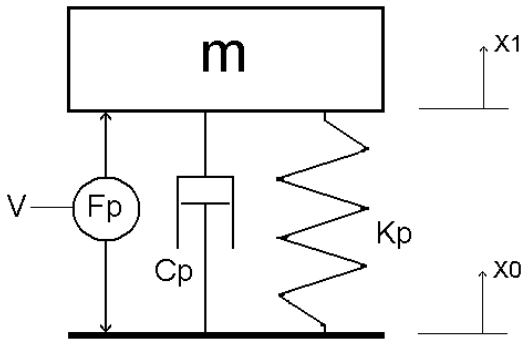

Figure 3. Thévenin equivalent model.

The Thévenin theory states that a vibration source can be represented at any particular frequency by an active force generator f_p, in parallel with a passive part of impedance Z_p (provided by a stiffness k_p and a damper c_p). Figure 3 shows the Thévenin equivalent model, where m is the load applied on THUNDER apex, f_p is a force generated by the piezoceramic element, k_p is its internal dynamical stiffness and c_p is its damping constant. With this model, we assume that the THUNDER is a linear system. Even with nonlinear effects, the Thévenin equivalent model has already been used for different actuators such as RAINBOW or C-Block [21], which have similar curvatures to the THUNDER.

In the classical Thévenin equivalent model, f_p is called the blocked force. This parameter is determined experimentally by measuring the force that is transmitted by the attachment point of the system to an infinitely rigid point. It is then possible to obtain the impedance by measuring the velocity of the attachment point (v_f) when the load connection is disconnected and perfectly free to move. The impedance Z_p is equal to f_p/v_f.

In the present analysis, a mechatronic approach [22] is used to extract the dynamic parameters of the THUNDER, including the actuator output force as a function of the external load. In other words, the modelling approach captures the feedback on the actuator due to the mass loading. In the case of the THUNDER actuator, the dynamic parameters are closely linked to its curvature, which in its turn is affected by the mass loading on the THUNDER apex. Therefore, this approach reflects more closely the real performance of the actuator, which is essential to optimize the design of the system. Based on the Thévenin equivalent model, the transfer function in Laplace form between the velocity $\dot{x}_1$ and the applied tension V is defined as follows:

$$\frac{\dot{x}_1}{V} = \frac{f_p}{ms^2 + c_p s + k_p}. \tag{1}$$

A second-order output-error (OE) model is used [23]. The OE model is composed of two parts: one corresponding to the system transfer function and the other considering the stochastical part comprising noise $e(t)$ in the measured signals. The latter is assumed to be white noise in laboratory conditions. A typical formulation of an OE model is as follows:

$$\dot{x}_1 = \frac{f_p}{ms^2 + c_p s + k_p} V + e(t). \tag{2}$$

The OE model is built from a state-space representation of the system to directly give the dynamic parameters, k_p, c_p and f_p, in the continuous time domain. Generally speaking, the identification process gives parameters in discrete time representation and it can be difficult to reach them in the continuous time domain. The state-space model is built from the typical differential equation of the Thévenin equivalent model:

$$m\ddot{x} + c_p\dot{x} + k_p x = f_p V. \tag{3}$$

The construction of the state-space model of the above equation yields

$$\begin{aligned} \dot{X} &= AX + BV \\ Y &= CX + DV \end{aligned} \tag{4}$$

where the state vector $X = (\dot{x}\, x)^T$ and

$$A = \begin{pmatrix} -\frac{1}{m}k_p & -\frac{1}{m}c_p \\ 0 & 1 \end{pmatrix} \quad \text{and} \quad B = \begin{pmatrix} \frac{f_p}{m} \\ 0 \end{pmatrix}.$$

C and D depend on the outputs of interest. In the identification process, the mass velocity is measured, so $D = (0)$ and $C = (1 \quad 0)$, with $Y = \dot{x}$.

The same experimental set-up, as presented earlier, was used to identify all the necessary parameters. Different masses were respectively applied on the THUNDER apex, as shown in figure 1. A B&K 3550 FFT analyser was used to generate a narrow white band excitation signal from 0 to 100 Hz. Ten thousand measuring points were acquired via a national instrument data acquisition board PCI-MIO-16E-4 with 300 Hz sampling frequency. The first five thousand points were used to identify different parameters and the rest were used for comparison and validation purposes. The parameters involved in the Thévenin model were obtained using the prediction error algorithm (PEM on an OE model) provided by a Matlab identification toolbox [23].

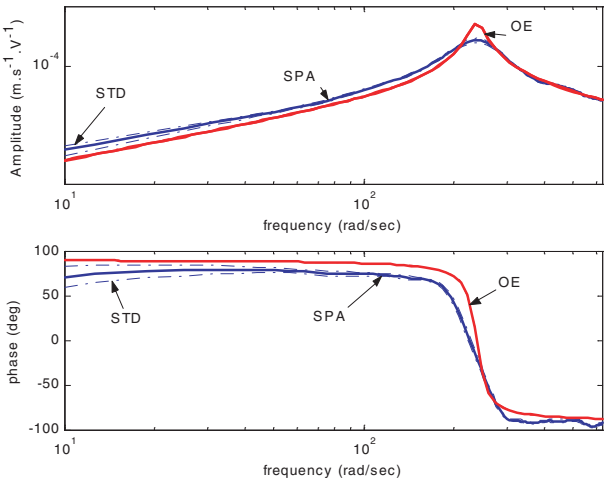

Figure 4. Bode diagrams of a THUNDER with a 750 g load on the apex. Comparison between SPA and the OE model computed using the PEM with associated STD.

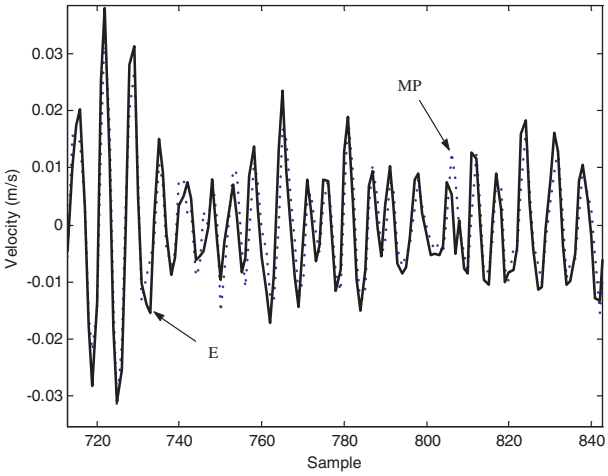

Figure 5. Comparison between the model prediction (MP) and experimental data (E) using a THUNDER with a 750 g load on the apex.

The transfer function obtained from parametric identification (OE model) is compared with that measured using spectral analysis (SPA). Figure 4 shows this comparison in terms of the Bode diagrams in the case of a THUNDER with a 750 g load. First of all, the identification shows that between 0–100 Hz, the THUNDER can be effectively considered as a secondary order system, as expected by the Thévenin equivalent model. Moreover, figure 4 shows that the spectrum from parametric estimation fits well with the results of SPA. Due to the use of a stochastical algorithm with white-noise excitation, standard deviations (STDs) can also be obtained. Different dot lines appearing in figure 4 represent these STDs.

It is important to validate the identification results using another totally independent set of data. This is done in figure 5 by comparing the time domain responses predicted by the model and those measured experimentally. Again, both sets of results achieve excellent agreement. In conclusion, both spectrum and time plots demonstrate that, under an appropriate identification, the Thévenin equivalent model gives a satisfactory prediction of the dynamics of the THUNDER below 100 Hz.

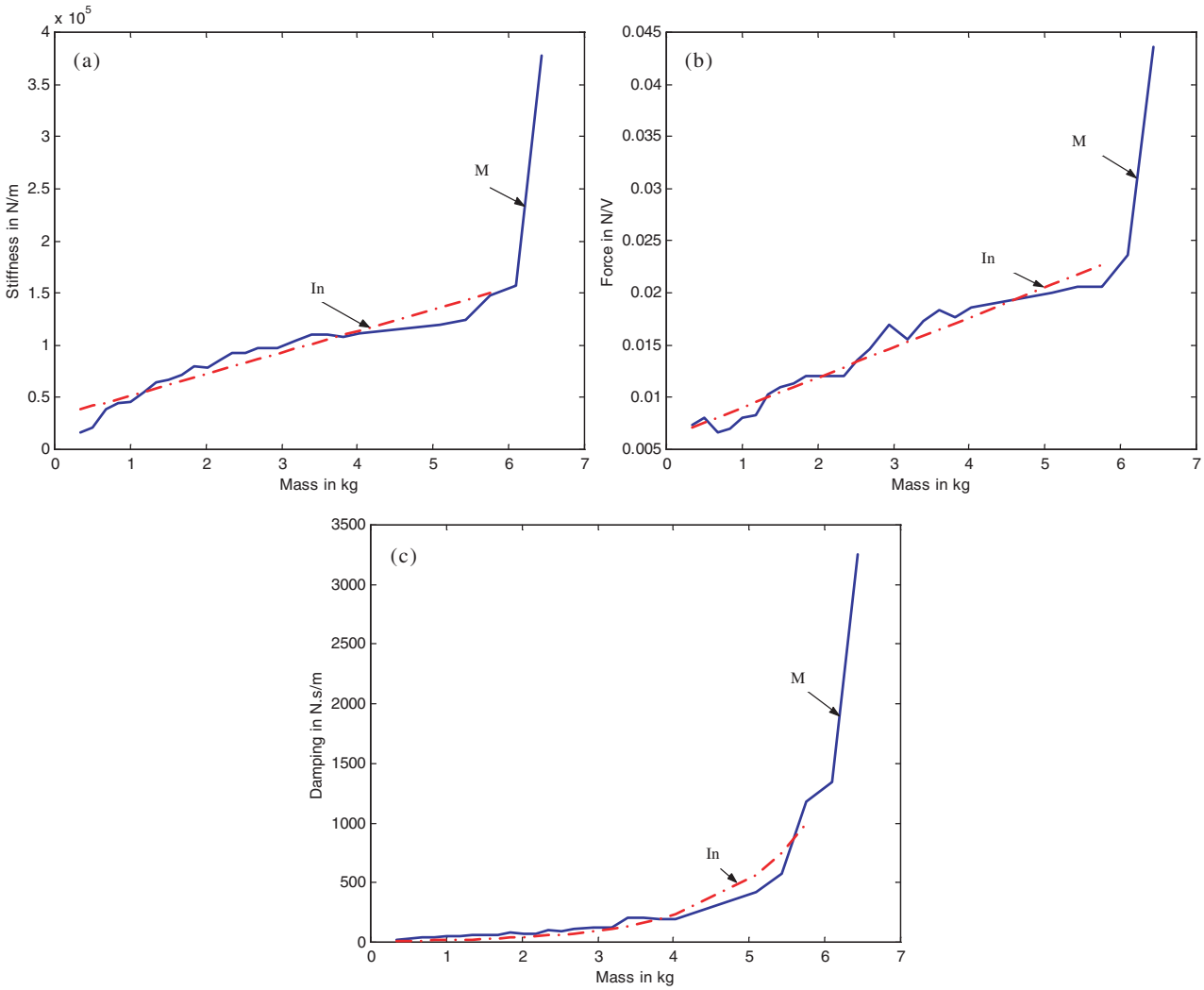

Figure 6. Comparison between the experimental results (M) and the interpolation curve (In) for: (a) dynamic stiffness versus mass loading; (b) block force versus mass loading; (c) dynamic damping versus mass loading.

It should be noted that the identified parameters using this approach are global parameters in the sense that the model includes the effect of the mass loading on the actuators. A series of tests following the aforementioned procedure was conducted to investigate the variation of these parameters with respect to mass loading. Masses varying from 250 g to 6.5 kg were respectively applied on the THUNDER apex. Figures 6(a)–(c) show the variation of stiffness, block force and damping, respectively. It can be noted that all three curves undergo reasonably smooth variation when mass loading is small. Drastic changes occur when the load attains 6 kg. In fact, when the load increases and eventually goes beyond a certain limit, the working condition of the actuators is rapidly deteriorated and the parameters used in the Thévenin model lose their physical meaning. This observation is consistent with information provided by the manufacturer, stating that the loading capacity of the THUNDER should be respected. Considering our application, the mass loading for each THUNDER is therefore limited to 5 kg. Regression analyses were then performed using these experimental data to represent the variation of each parameter. Linear interpolation is found to be sufficient to use for the stiffness and the blocking force and an exponential function is used in the case of damping. Detailed mathematical expressions are as follows:

$$\begin{aligned} &\text{Stiffness: } k_p = 20\,619m + 31\,217 \\ &\text{Blocking force: } f_p = 0.0028m + 0.006 \\ &\text{Damping: } C_p = 8.018\mathrm{e}^{0.836m}. \end{aligned} \tag{5}$$

These relationships are used both for simulation and controller design.

Some remarks are needed to outline some particular behaviour of the THUNDER. As illustrated in figure 4, when excited by a narrow-band white-noise signal, a THUNDER actuator behaves basically like a second-order system. During experiments, however, it was found that a highly nonlinear behaviour might occur at some particular frequencies. In fact, similar observations have been made in a NASA test with a 50 g load [15]. Using the same configuration, tests performed in our laboratory using harmonic excitation with various frequencies confirm these observations. Another problem related to the use of the THUNDER is the ageing problem. In fact, after frequent tests during a period of time, its characteristic properties, including curvature and dynamic properties, can

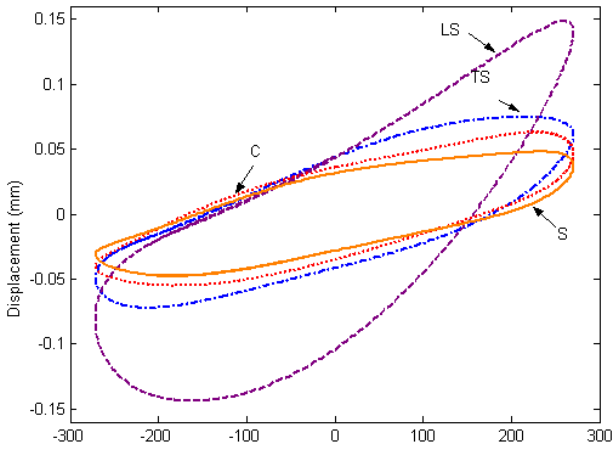

Figure 7. Displacement versus voltage of a THUNDER used for one week under different boundary conditions: TS, tight screw; LS, loose screw; C, clamped; S, silicone gels (200 V rms harmonic excitation applied to the THUNDER at 15 Hz with 500 g on the THUNDER apex).

have appreciable changes. A typical result is given in figure 7, which shows the variation of THUNDER displacement with respect to the applied voltage. The tests were conducted in a similar way as in figure 2 but after one week of extensive use. Comparing with figure 2, it can be seen that the displacement of the THUNDER is generally reduced, although conclusions drawn previously concerning the boundary conditions still apply. Even with these disadvantages, the model developed above can still provide a valuable vehicle for the system design and can provide reasonable tolerance for considering the parameter variation.

4. Control simulations and experiments

An isolation prototype was designed and manufactured. The Thévenin model developed above was used to perform numerical simulations during the controller design. Finally, experiments were carried out. Both numerical and experimental results that are presented hereafter are obtained using the prototype.

Figure 8(a) shows the whole system with a closer look at the THUNDER installation in figure 8(b). Basically, the prototype is composed of three triangular plates with three guide rods passing through each corner. The bottom plate which is rigidly mounted on a metallic frame is used as a fixture. The plate in the middle is excited by a shaker and serves as a vibration source. The plate is referred to as the lower vibrating plate (LVP) hereafter. Three THUNDERs are mounted on top of this plate and used as isolators (figure 8(b)). Another plate is then placed on top of the actuators. This plate represents the structure to be isolated and is called the receiving plate. Different masses and an accelerometer are then put on top of the receiving plate. The system to be controlled may be approximated by a single-degree-of-freedom system.

A simple feedback controller has been chosen because it is the best approach in situations where it is not possible to sample the incoming disturbance soon enough for a feedforward control system to be effective [16]. A classical feedback controller on acceleration [24] is used (figure 9). The feedback sensor is an accelerometer, and the active force generated by the THUNDER, f_p, is proportional to the feedback signal coming from the accelerometer. The feedback voltage is generated using a gain factor g_a as follows

$$V = -g_a(\ddot{x}_0 + \ddot{x}_1) \tag{6}$$

where $\ddot{x}_0$ is the acceleration of the LVP and $\ddot{x}_1$ is the relative acceleration of the receiving plate with respect to the LVP. Under these conditions, the closed-loop response of this system is obtained using the following dynamic equation:

$$m(\ddot{x}_0 + \ddot{x}_1) = -g_a(\ddot{x}_o + \ddot{x}_1) f_p V - c_p \dot{x}_1 - k_p x_1. \tag{7}$$

The transfer function between the mass acceleration and the input acceleration in the Laplace domain is

$$\frac{\ddot{x}_0 + \ddot{x}_1}{\ddot{x}_0} = \frac{c_p s + k_p}{(m + f_p g_a)s^2 + c_p s + k_p}. \tag{8}$$

The effect of feedback acceleration is clearly dependent on the effective mass of the whole system. The stability of the closed-loop system is ensured, provided $m + f_p g_a$ is positive, as shown by the Routh–Hurwitz criterion. Among other physical parameters, the gain factor g_a plays an important role in determining the closed-loop natural frequency of the system. Also, the latter can, in principle, be arbitrarily chosen by adjusting the gain factor; in practice however various factors, such as noise and sensor resolution, limit the range over which the properties of such a mechanical system can be modified by feedback control. This is discussed later in the experimental section. In aeroplanes, the natural frequency of the isolation would be properly set to achieve effective isolation between the feet of passengers and the floor. In this case, it is important to consider the resonances of feet depending on knee angles [25]. In designing our controller in the present case, the closed-loop natural frequency is maintained under 20 Hz.

Using the Thévenin equivalent model developed previously, simulations have been made to predict active isolation performance. Following the procedure outlined in the system identification section, a numerical simulator was developed using Matlab with Simulink in the form of state-space representation. A typical simulation is presented in figure 10, in which we compare the power spectra of the receiving plates with and without control. In this simulation, a 1.5 kg mass was put on the receiving plate and g_a was set to be 314 V $(\mathrm{m\ s^{-2}})^{-1}$. The effect of acceleration feedback can be clearly seen from the shift of the natural frequency of the system. Higher-frequency accelerations are therefore more effectively attenuated. Since no velocity feedback was used to increase damping, amplification can be noticed around the resonance [24].

Another interesting case to investigate is the multi-harmonic excitations. In typical turboprop aircraft, strong vibrations have been observed at frequencies corresponding to the blade-passage frequencies of the propellers. Multi-harmonic excitations at 70, 140 and 210 Hz were therefore investigated. Again, using a 1.5 kg load and a gain factor of 314 V $(\mathrm{m\ s^{-2}})^{-1}$, the time domain response of the receiving plate is presented in figure 11. One can notice that, once the controller is turned on, the plate vibration is effectively attenuated within a very short time. It should be noted that both figures 10 and 11 show only the active part of the isolation.

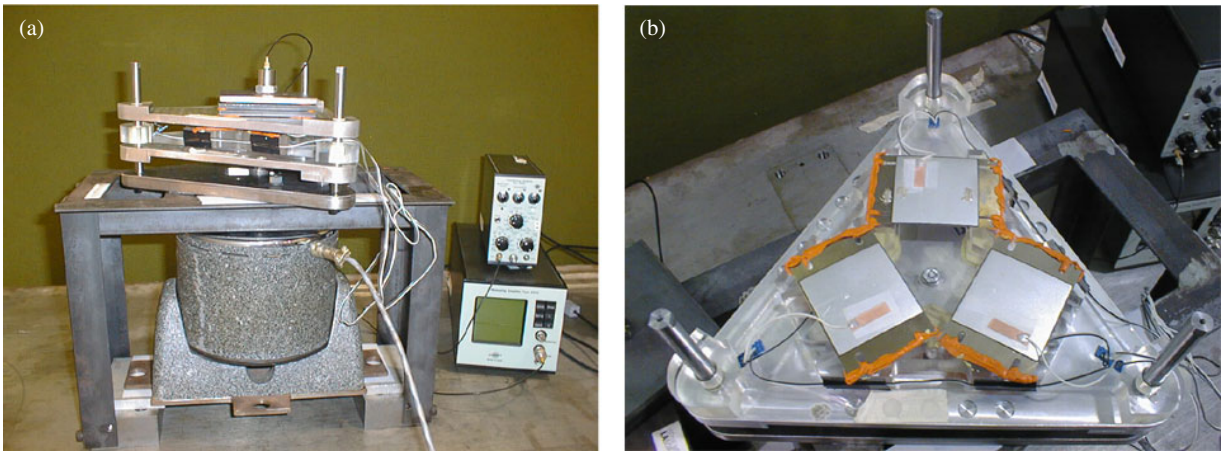

Figure 8. (a) Isolation prototype using the THUNDER. (b) THUNDER installation.

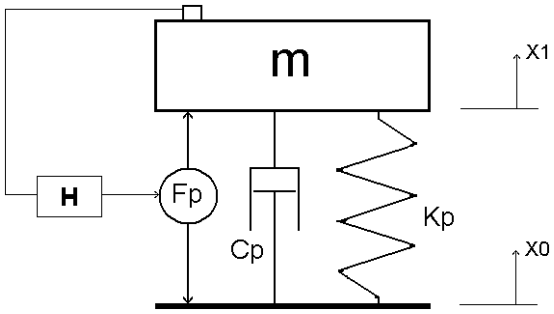

Figure 9. Feedback control on acceleration.

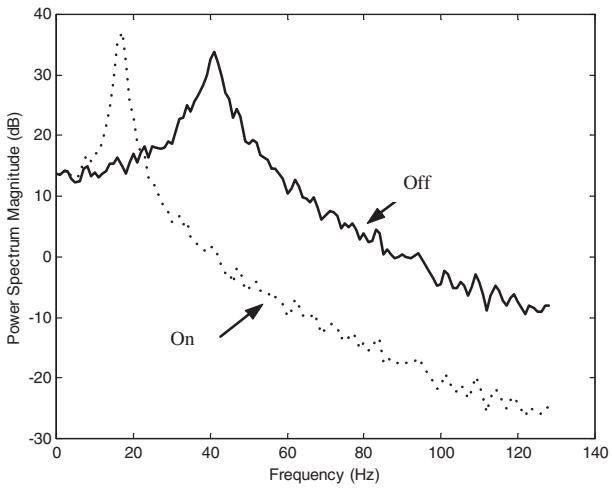

Figure 10. Simulated power spectra of the acceleration of the receiving plate with a 1.5 kg mass mounted on three THUNDERs with and without control.

The passive effect of the THUNDER had been incorporated before the controller was turned on.

On the basis of simulation results, an analogue controller was designed and implemented on the isolation prototype. As mentioned before, in simulation g_a can be chosen to reach whatever natural frequency desired. In practice, however, a very low-frequency isolation system is very difficult to obtain. A low-frequency system would require a high feedback gain factor to achieve high isolation. As a result, the system tends

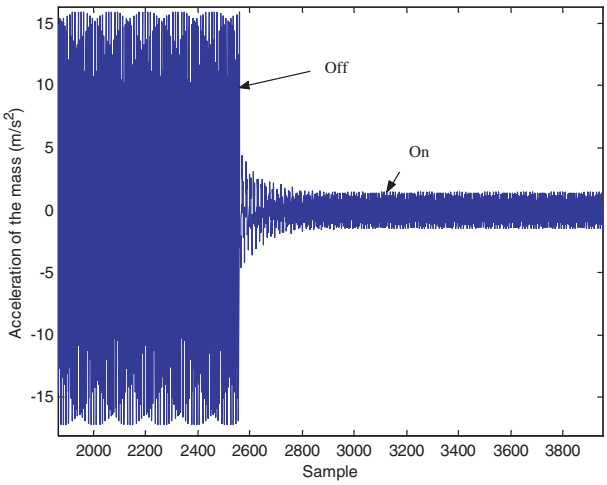

Figure 11. Acceleration of the receiving plate in the time domain under multi-harmonic excitations.

to be less stable and any unpredictable factors, such as signal noise, unexpected external disturbance and nonlinearity of the system, would make the system unstable. During experiments, g_a is set to 314 V $(\mathrm{m\,s^{-2}})^{-1}$ to obtain natural frequency at 17 Hz with 1.5 kg on the top plate. The whole system can be seen in figures 8(a) and (b). Concerning the control loop, a B&K 4338 accelerometer was used as feedback sensor and a B&K 2525 measuring amplifier was used to change the gain in the loop. A first-order RC low-pass filter was also used to eliminate high-frequency components in the feedback signal and noise. For performance assessment, an independent laser vibrometer was used to measure the vibrations of both plates to which only an anti-aliasing filter was used for data processing. The cut-off frequency was much higher than the highest frequency presented in the results.

Figure 12 shows the power spectra of the receiving plate with a 1.5 kg load before and after control. The effect of the controller is significant in the range of 30–100 Hz. Due to the damping of the system, amplification corresponding to the system resonance is not as apparent as that predicted in simulation with zero damping. The analogue controller changed the natural frequency of the system from 41 to 17 Hz, whilst the model predicted 18 Hz.

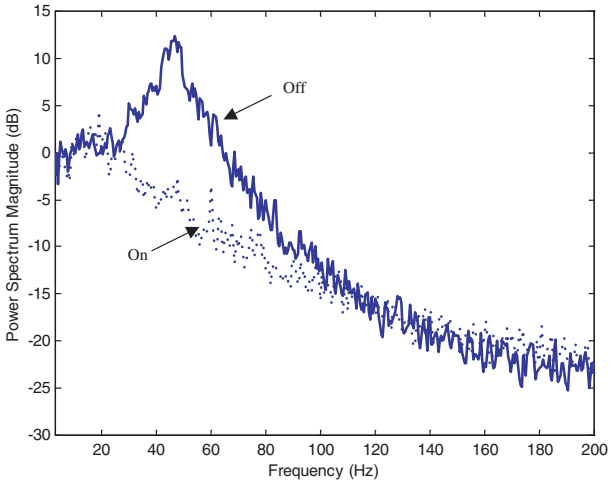

Figure 12. Experimental results on the power spectra of the acceleration of the receiving plate with a 1.5 kg mass mounted on three THUNDERs.

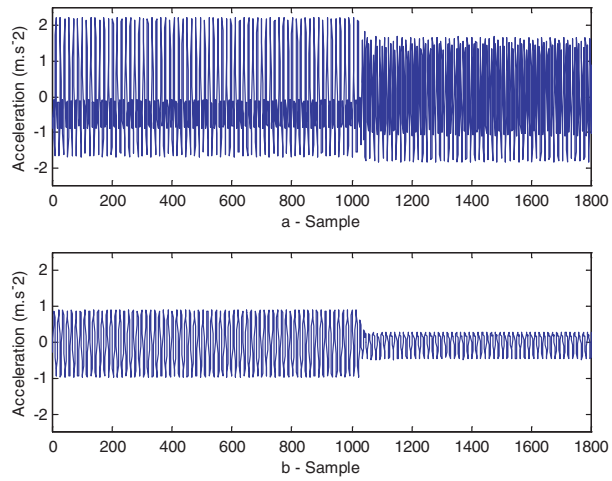

Figure 13. THUNDER effects on the LVP and the receiving plate. Experimental results under multi-harmonic excitation: (a) LVP, (b) receiving plate.

It should be noted that THUNDER actuators provide both passive and active isolation. The actuator flexibility induces passive isolation and the controller provides the active isolation. Using multi-harmonic signals, the effects of the THUNDER actuators on both plates are illustrated in figure 13. The top part of the figure shows the acceleration power spectrum density (PSD) of the LVP and the lower part shows the PSD of the receiving plate. It can be seen that, before the controller is turned on, the vibration of the receiving plate is weaker than the vibration of the lower plate due to the passive effect of the THUNDER. Among the three frequency components (70, 140 and 210 Hz), 70 Hz is the most difficult to be isolated by the passive effect. Once the controller is on, the acceleration of the receiving plate is further reduced.

Finally, figure 14 allows a better assessment of the global isolation effect. In this figure, the acceleration power spectra of both plates are compared. It is noticed that the use of THUNDER actuators offers a very effective isolation effect.

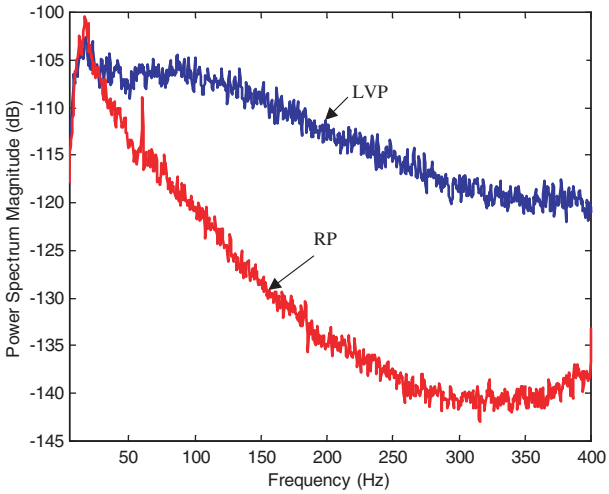

Figure 14. PSD of acceleration of the LVP and the receiving plate (RP).

The global attenuation is quite obvious over a wide range of frequencies. When placing hands on both plates, one can clearly feel the difference.

5. Conclusions

In this paper, we focus on the simulation, design and experimental tests of an isolation system using the newly developed THUNDER actuators. Basically, it is a feasibility study applying a new type of actuator to a classical vibration problem. The main finding of this research can be summarized as follows:

(1) The THUNDER provides an ideal actuator in the isolation of lightweight mechanical components. Apart from the classical passive effect due to the flexibility, a simple feedback controller can greatly enhance the isolation performance due to its high displacement property. Any other well-established analogue or digital controllers can certainly improve the control performance.

(2) A practical way of installing a THUNDER actuator is to use silicon gel at both ends, preventing such skipping whilst generating the highest displacement.

(3) A simple Thévenin equivalent model can be used to model the dynamic behaviour of the mass loaded THUNDER. Under reasonable weight and within the scope of the design, empirical correlation representing variations of dynamic parameters can be established for predicting physical parameters of the THUNDER. These relationships are simple and accurate enough to be used in the controller design and the control performance prediction.

Our future work will focus on the installation of an active system in aircraft floors using the THUNDER. Since the concept feasibility is assessed in this paper, a more sophisticated and powerful adaptive controller may be necessary to enhance the control performance. Indeed, preliminary tests on a Dash-8 floor panel using 4×4 feedforward control has already shown some very good results.

Acknowledgments

This work was supported by Structure R&D, Bombardier Aerospace in Toronto and National Science and Engineering Research Council of Canada. It was also supported in part by a grant from the Research Grants Committee of the Hong Kong SAR (grant no PolyU 5155/01E).

References

[1] Wlezien R W, Horner G C, McGowan A R, Padula S L, Scott M A, Silcox R J and Simpson J O 1998 The aircraft morphing program *39th Structures, Structural Dynamics and Materials Conf. and Exhibit AIAA* 98-1927 pp 1–13

[2] Larson C R, Falangas E, Dobbs S K, Neurgoankar R R, Nelson J G, Rosenthal J S, Hustedde C L and McGrath S F 1998 Piezoceramic active vibration suppression control system development for the B-1B aircraft *SPIE Industrial and Commercial Applications of Smart Structures Technologies* pp 294–305

[3] D'Cruz J 1998 Active suppression of aircraft panel vibration with piezoceramic strain actuators *J. Aircr.* **35** 139–44

[4] Proulx B and Cheng L 2000 Dynamic analysis of piezoceramic actuation effects on plate vibrations *Thin-Walled Struct.* **37** 147–62

[5] St-Amant Y and Cheng L 2000 Dynamic modeling and analysis of plate vibration with integrated piezoceramic elements *Thin-Walled Struct.* **38** 105–23

[6] Henry J K and Clark R L 1999 A curved piezo-structure model: Implication on active structural acoustic control *J. Acoust. Soc. Am.* **106** 1400–7

[7] Shakeri C, Noori M N and Hou Z 1997 Smart materials and structures a review *Proc. 4th Int. Conf. on Civil Engineering (Sharif University of Technology, Tehran, Iran May) Paper no* 9513 pp 312–28

[8] Brennan M J, Garcia-Bonito J, Elliot S J, David A and Pinnington R J 1999 Experimental investigation of different actuator technologies for active vibration control *Smart Mater. Struct.* **8** 145–53

[9] Habibi S and Goldenberg A A 1999 Design and analysis of a new symetrical linear actuator for hydraulic and pneumatic systems *Trans. Can. Soc. Mech. Eng.* **23** 377–96

[10] Maier R 1999 Helicopter interior noise reduction by active vibration isolation with smart gearbox struts *Active 99* **1** 189–98

[11] Madden J D, Cush R A, Kanigan T S and Hunter I W 2000 Fast contracting polypyrrole actuators *Synth. Mater.* **113** 185–92

[12] Ghandi K and Hagood N W 1994 Shape memory ceramic actuation of adaptive structures *Proc. AIAA/ASME Adaptive Struct. Forum (Hilton Head, SC, USA) AIAA paper no* 94-1758

[13] Yoon K J, Shin S, Park H C and Goo N S 2002 Design and manufacture of a lightweight piezo-composite curved actuator *Smart Mater. Struct.* **11** 163–8

[14] Malowicki M and Leo D J 2001 Active vibration isolation using an induced strain actuator with application to automotive seat suspension *Shock Vib.* **8** 271–85

[15] Copeland B M, Buckley J D, Bryant R G, Fox R L and Hellbaum R F 1999 THUNDER—an ultra-high displacement piezoelectric actuator *NASA Langley Research Center* (Hampton, VA) 23681-0001

[16] Hansen C H and Snyder S D 1996 *Active Control of Noise and Vibration* (London: Spon)

[17] Pinkerton J L, McGowan A R, Moses R W, Scott R C and Heeg J 1996 Controlled aeroelastic response and airfoil shaping using adaptive materials and integrated systems *Proc. SPIE Smart Struct. Integr. Syst.* **2717** 166–77

[18] Hixson E L 1987 *Mechanical Impedance Shock and Vibration Handbook* 3rd edn (New York: McGraw-Hill) ch 10

[19] Song J K and Washington G 1999 THUNDER actuator modeling and control with classical and fuzzy control algorithm *Proc. SPIE Smart Struct. Integr. Syst.* **3668** 866–77

[20] Taleghani B K and Campbell J F 1999 Non-linear finite element modeling of THUNDER piezoelectric *Proc. SPIE Smart Struct. Integr. Syst.* **3668** 555–66

[21] Garcia-Bonito J, Brennan M J, Elliott S J, David A and Pinnington R J 1998 A novel high-displacement piezoelectric actuator for active vibration control *Smart Mater. Struct.* **7** 31–42

[22] Gilbert M G and Horner G C 1998 Actuator concepts and mechatronics *SPIE Industrial and Commercial Applications of Smart Structures Technologies* pp 214–22

[23] Ljung L 1999 *System Identification—Theory For the User* 2nd edn (Englewood Cliffs, NJ: Prentice-Hall)

[24] Fuller C R 1997 *Active Control of Vibration* (New York: Academic)

[25] Kitazaki S 1997 The apparent mass of the foot and prediction of floor carpet transfer function *United Kingdom Group Meeting on Human Response to Vibration (ISVR, University of Southampton)* pp 355–67